Int. J. Nanosci. Nanotechnol., Vol. 20, No. 1, March 2024, pp. 11-23
DOI: 10.22034/ijnn.2024.561301.2268

Green Synthesis of Iron Nanoparticles using Eucalyptus Leaf Extracts and Characterization for Photocatalytic Studies

V. K. M. Katta[1], R. S. Dubey[2] and Sigamani Saravanan[1,*]

[1]Department of Science & Humanities, Swarnandhra College of Engineering & Technology (A), Seetharampuram, Narsapur (W.G.), Andhra Pradesh, India
[2]Department of ECE, University Institute of Engineering & Technology, Guru Nanak University, Ibrahimpatnam, RR District (TL), India

(*) Corresponding author: shasa86@gmail.com
(Received: 02 September 2022 and Accepted: 23 February 2024)

Abstract

The simple and free solvent green synthesis approach is promising for the preparation of nanoparticles due to its eco-friendly and straightforward, which replaced the use of toxic chemicals. This work reports the synthesis of iron nanoparticles using the eucalyptus leaf extracts and it has been studied their structural, functional groups, morphological, and elemental properties. Initially, X-ray diffraction (XRD) pattern showed the presence of organic materials and iron (α-Fe phase). Next, Fourier transform infrared (FTIR) and Raman spectroscopy (RS) were confirmed the presence of iron oxide (Fe-O) stretching vibrations at 550 cm-1 and 575 cm^{-1}, respectively. The UV-visible absorbance spectrum endorsed the existence of the plasma enhancement in between 250 to 370 nm, and scanning electron microscopy (SEM) micrographs shown the formation of irregular spherical grains. The energy-dispersive X-ray spectroscopy (EDX) investigation was evidenced the presence of iron (Fe) nanoparticles. Finally, the successful preparation of iron nanoparticles used as the catalyst for the photo degradation (~98% for 150 min.) study of Rhodamine B dye and results discussed.

Keywords: *Green synthesis, Eucalyptus leaf, Iron nanoparticles, Plasmon, UV-absorption.*

1. INRODUCTION

Green synthesis of iron (Fe) nanoparticles has been attracting and garnered large attention due to their best alternative over the conventional methods, which are eco-friendly to the environment and non-toxic approach. In recent years, several works report using green synthesis process by using the plant extracts. Fahmy et al. reviewed the synthesis of Fe nanoparticles using the tea extracts (Oolong tea, tea powder, tea waste, tea polyphenols etc.) and other plant extracts like Amaranthus dubius, Murray coinage, eucalyptus etc. These nanoparticles addressed for their potential applications in dye and contamination removal, anti-bacterial agent [1]. *Jeevanandam et al.* demonstrated the biosynthesis of MgO nanorods using eucalyptus globules leaf extracts. The obtained results showed the significant rod-shaped nanoparticles having superior cellular penetration than the other structures. Further, they suggested the usage of these nanorods in various medical applications [2]. *Kata and Dubey* synthesized silver nanoparticles using extracts of Tagetes erect plant and investigated their structural, optical, chemical and morphological character-istics. The prepared silver nanoparticles exhibited the decreased quantum confinement effect and yielded the photocatalytic activity [3]. *Sundararajan et al.* presented the pristine and cobalt ferrite doped zinc ($CO_{1-x}Zn_xFe_2O_4$) nano-structured materials using the microwave combustion method for photocatalytic degradation of Rhodamine B. Among various prepared nanostructures, $Co_{0.6}Zn_{0.4}Fe_2O_4$ showed 99.9%

degradation efficiency using irradiation of visible light [4]. *Varadavenkatesan et al.* presented the green synthesis of ZnO nanoparticles with cyanometraramiflora leaf extracts for photodegradation of Rhodamine B dye. They found it improved degradation efficiency of 98% under sunlight irradiation and maintaining a constant degradation of dye in about 0.017/minutes [5]. *Yi et al.* presented the green synthesis of iron (Fe) nanoparticles using nephrolepis auriculata. The transmission electron microscopy (TEM) and X-ray diffractometer (XRD) confirmed the formation of spherical shaped nanoparticles with their sizes of 40-70 nm while XRD investigation showed amorphous nature. The presence of organic acids, flavonoids and polyphenols also revealed by the Fourier- transform infrared (FTIR) spectroscopy measurement. The prepared nanoparticles were used for waste water treatment and they noticed the removal of 90.93% of chromium [6]. *Mo et al.* prepared the silver nanoparticles using eucalyptus leaf extracts and studied their UV-absorbance, structural, morphological, and functional group properties. The field-emission transmission electron microscopy (FESEM) revealed the spherical silver nanoparticles with their sizes from 4 to 60 nm. The FTIR spectroscopy analysis confirmed the presence of polyphenols and proteins, which acted, as reducing and stabilizing agent [7]. *Wang et al.* synthesized the iron (Fe) nanoparticles using the eucalyptus leaf and characterized by various techniques. The scanning electron microscopy (SEM) and X-ray energy-dispersive spectrometer (EDX) revealed the spherical morphology and usual elements present in the sample. The prepared iron nanoparticles mixed with swine wastewater, and they observed about 84.5% of chemical oxygen demands. They suggested these nanoparticles have tremendous potential in situ remediation of eutrophic wastewater [8]. *Vitta et al.* reported the green synthesis of iron nanoparticles from the eucalyptus robusta Sm for antioxidant and antimicrobial activities. They maintained the proportion of leaf extract and iron salt during the tests. The antimicrobial activity studied for various microorganisms and the antimicrobial activity found with the prepared iron nanoparticles [9]. *Wang* presented the synthesis and characterization of iron-polyphenol complex nanoparticles using eucalyptus leaf extracts. The TEM morphological investigation revealed the particle size from 40 to 60 nm. The adsorption-flocculation capacity for acid black 194 noticed with 1.6 grams of complex nanoparticles at room temperature [10]. *Weng et al.* prepared the bimetallic (Fe/Ni) nanoparticles using eucalyptus leaf extracts. The FTIR and thermogravimetric analysis (TGA) spectrum evidenced the presence of various biomolecules. The particle sizes were found to vary from 20-50 nm confirmed by SEM. The EDX spectroscopy peaks of iron as and [11]. Overall, the green synthesized nanoparticles have some drawbacks such as heterogeneous sizes, shapes and agglomerated structures. Also, plant extract based green synthesized nanoparticles are eco-friendly, stable, easy to prepare and economical methods [12].

In this paper, we present the green synthesis of iron nanoparticles using eucalyptus leaf extracts, which was acting as reducing and capping agent. The prepared sample investigated for their optical, structural, morphological, elemental and functional groups using various characterization techniques. Finally, the Photocatalytic performance investigated with respect to the various times.

2. EXPERIMENTAL APPROACH

2.1. Materials and Methods

The ferrous sulfate ($FeSO_4.7H_2O$), de-ionized water, eucalyptus leaf and, filter papers are the primary materials to carry out this work. Initially, the ferrous sulfate (crystalline, 99% purity) was used as the

source of the iron and whereas de-ionized (DI) water was used as the solvent. The eucalyptus leaf extracts used as capping and stabilizing agent for the preparation of iron (Fe) nanoparticles.

2.2 Synthesis of Nanoparticles (NPs)

Figure 1 shows the experimental procedural steps for the preparation of iron (Fe) nanoparticles. At first, the fresh eucalyptus leaves collected and washed several times by using DI water and then naturally dried in sunlight for 24 hrs. After that, the dried eucalyptus leaf crushed into smaller pieces. The crushed leaves of 15 grams were soaked in 250 nm DI water and boiled at 80°C for 1 hour by using the magnetic stirrer.

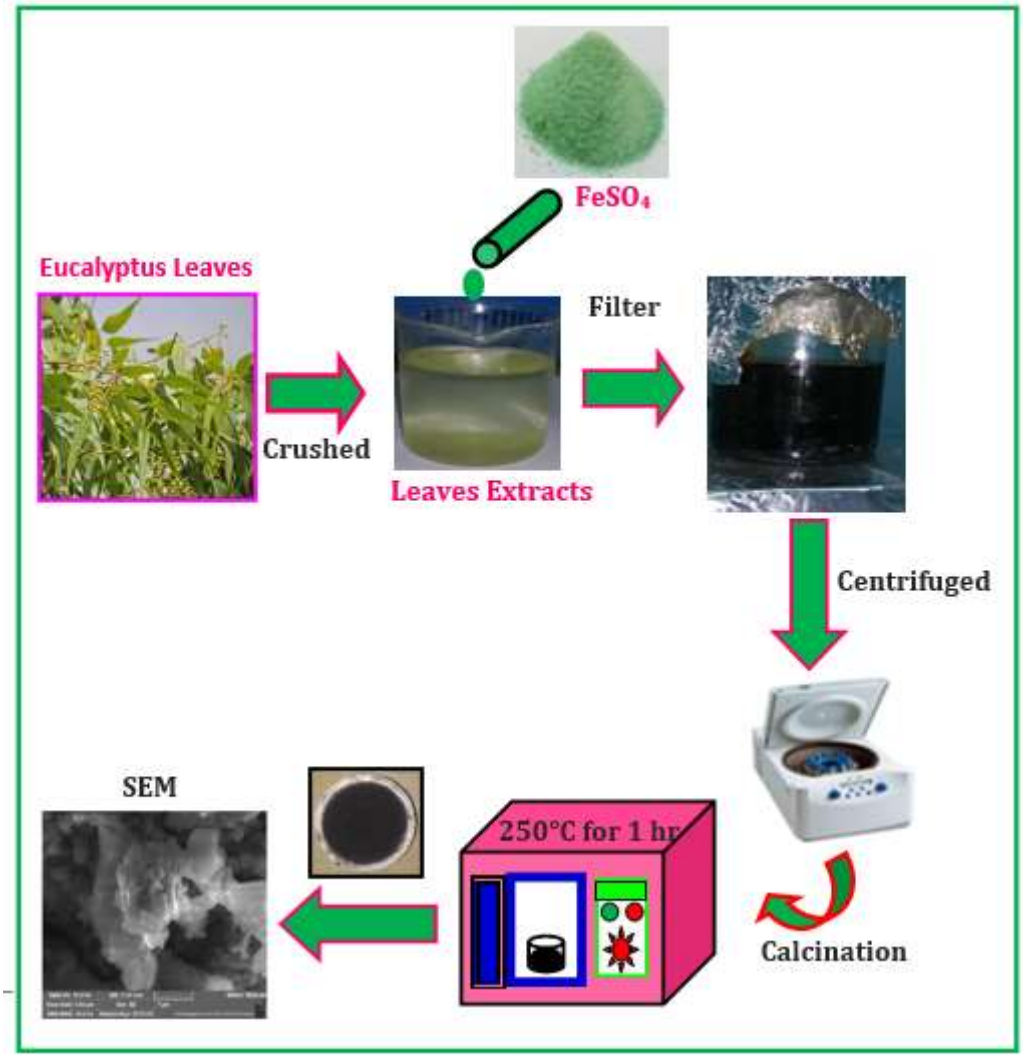

Figure 1. *The green synthesis process of iron nanoparticles.*

The plant residuals were filtered using Whatman filter paper after the natural cooling is of the extracts. To extract iron nanoparticles, 200 ml of above prepared extracts mixed with 2:1 of 0.1 M of $FeSO_4$ at room temperature. After adding $FeSO_4$, the black color solution was appeared which confirmed the reduction of Fe^{2+} ions (Wang et al., 2013).

Finally, the particulate collected by using the filtration and centrifugation process (3000 rpm) for 15 minutes and later the sample was dried in hot-air oven. Finally, calcination of the prepared sample

done at a temperature 250°C for 1-hour using muffle furnace.

2.3 Characterization of Nanocatalyst

The prepared nanoparticles were characterized using the XRD (Bruker D8, Venture), FTIR (Perkin Elmer-Spectrum Two, US), UV-Visible (Shimadzu, UV-1800), Raman (Horiba Scientific, Japan), SEM (MIRA3 TESCAN, Czech Republic) and EDX (Oxford X-Max 50, Germany). It was useful for examining the crystallinity, functional groups, UV absorbance, morphology and elemental composition of the present in the sample. Further, the prepared nanoparticles used as catalyst to study the photo-degradation of Rhodamine B dyes.

2.4 Photocatalytic Degradation

The iron nanoparticles (30mg) dispersed in a 100 ml of a Rhodamine B dye solution with the concentration of (30mg/L) in 100 ml borosil beaker to know the photodegradation. Before the light irradiation process, the RhB solution was prepared and maintained by the absence of light for the adsorption or desorption. Next, these mixture solution were kept under UV-Visible light lamps (around 400 nm) for the irradiation of visible light.

3. RESULTS AND DISCUSSION

3.1. X-Ray Diffraction (XRD)

Using the green synthesized method, the prepared iron nanoparticles investigated using X-ray diffraction technique. The X-ray diffraction pattern of iron nanoparticles presented in **Figure 2.** The XRD measurement was carried out in the range from 2θ= 10 to 80°. One can notice the presence of various diffraction peaks which indicate the formation of iron nanoparticles.

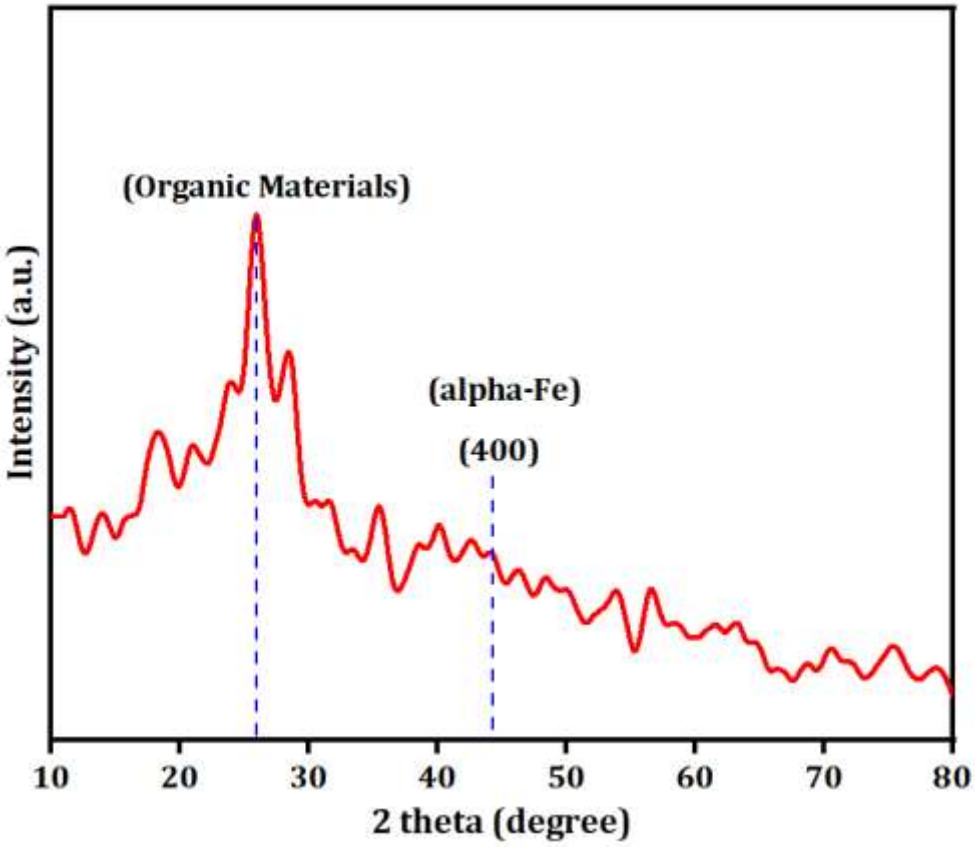

Figure 2. *XRD diffraction pattern of iron nanoparticles.*

The broader shoulder peak originated at 2θ=25.84° was identified as the adsorption of organic materials from the eucalyptus leaf extracts, which serves as capping and stabilizing agent [8, 13-14]. The similar peaks were noticed in other reported works [6, 15-16]. The small peak observed at 2θ= 44.3° corresponding to the plane (400) can be regarded to the presence of α-Fe as reported by various researchers [8, 13, 16-19]. Also, the reduction of 'Fe' peak intensity may be due to the difference in the electron densities of the host materials and depending on the various parameters such as structure, scattering factor, etc. [20, 21].

3.2 Scanning Electron Microscopy (SEM)

As shown in **Figure 3**, the scanning electron microscopy (SEM) micrographs reveal the agglomerated iron nanoparticles. The synthesized iron nanoparticle seems to be a spherical shape with their irregular shape. Noticeably, the iron nanoparticles tend to agglomerate between the interparticles contact, adhesiveness, and magnetic interactions. Accordingly, the biomolecular derived from the eucalyptus leaf extracts considered as capping on Fe nanoparticles and act as stabilizing agents. Further, these biomolecules reduced the electrostatic repulsion and steric hindrance [13, 8, 36, 37].

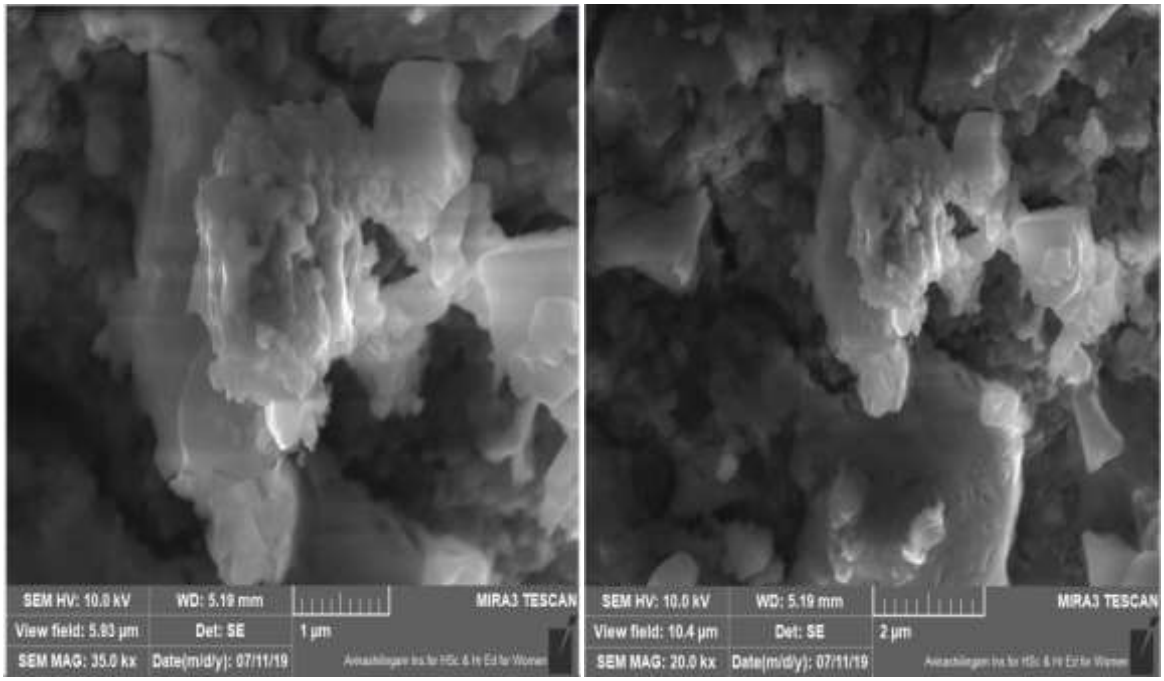

Figure 3. *SEM morphological image of iron nanoparticles.*

3.2. Fourier Transform Infra-Red Spectroscopy (FTIR)

Fourier transforms infra-red (FTIR) spectroscopy investigation was performed to know the functional groups of the prepared metal precursors and capping agent as shown in **Figure 4.** The FTIR transmittance spectrum plotted in the range of 400 to 4000cm^{-1}. This result indicates the presence of various functional groups in the eucalyptus extracts which include polyphenols, and organic acids [22]. These functional groups were responsible in the reduction of Fe^{3+} and acted as capping on the iron nanoparticles. The synthesized Fe nanoparticles' using the plant extracts demonstrates the weak transmittance peaks as can be noticed. The Fe-O stretching mode was presented at 583 cm^{-1} (inset figure 4). As can be seen in **Figure 4**, the

absorption band originated at 3473 cm^{-1} can be attributed to the O-H stretching mode [8].

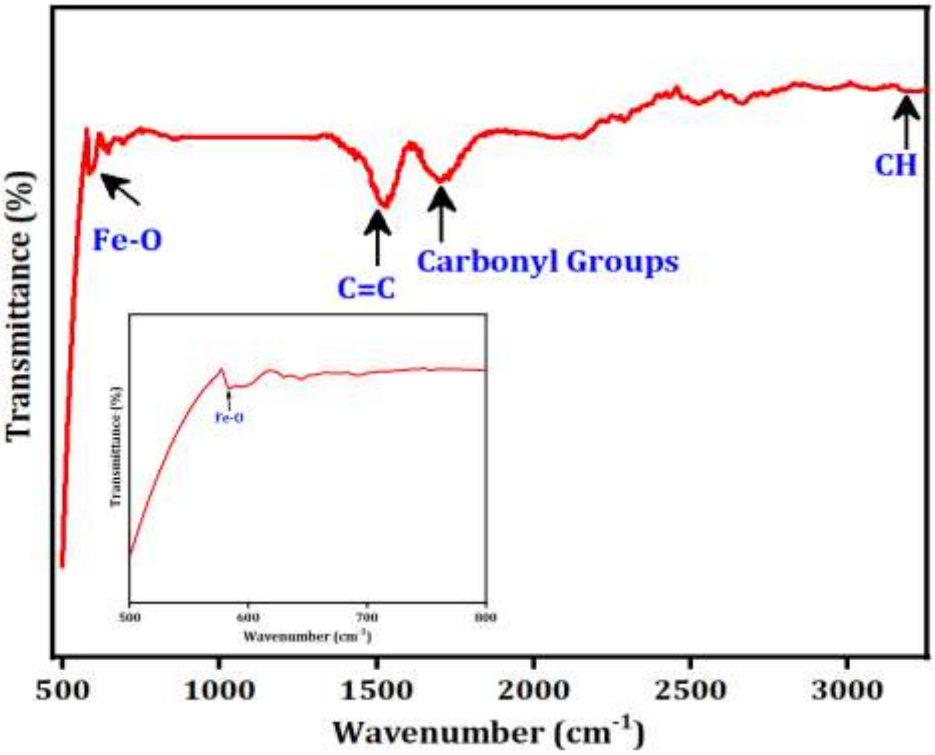

Figure 4. *FTIR transmittance spectrum of iron nanoparticles.*

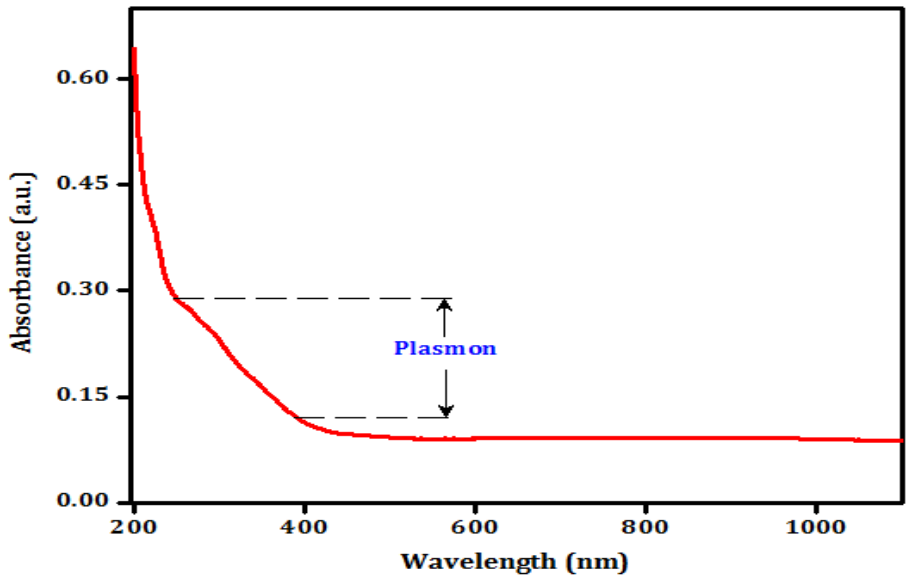

Figure 5. *UV-visible absorbance spectrum of iron nanoparticles.*

Another band at 2926 cm^{-1} was found related to the CH and CH_2 vibration modes (aliphatic hydrocarbons) while a band at 1700 cm^{-1} was ascribed to the presence of carbonyl groups [23]. The broad band from 1456 to 1610 cm^{-1} was attributed to the phenolic compounds of the eucalyptus leaf extracts (C=C aromatic ring stretching vibration modes). These polyphenols noticed and bounded on the iron nanoparticles and stabilized by interacting with the free carboxylic groups [24]. Further, another band noticed at 550 cm^{-1} can be referred to the stretching of iron oxides (Fe_2O_3 or Fe_3O_4) [25].

3.4. UV-Visible Spectroscopy (UV-Vis)

Figure 5 shows the UV-vis absorbance of the green synthesized iron nanoparticles, which dominantly shows the plasma properties. A plasmon enhancement band can be observed from 250 to 370 nm. The absorbance spectrum shows the similar nature as reported in the literature and the band originated at 360 nm corresponds to the iron nanoparticles [26-28].

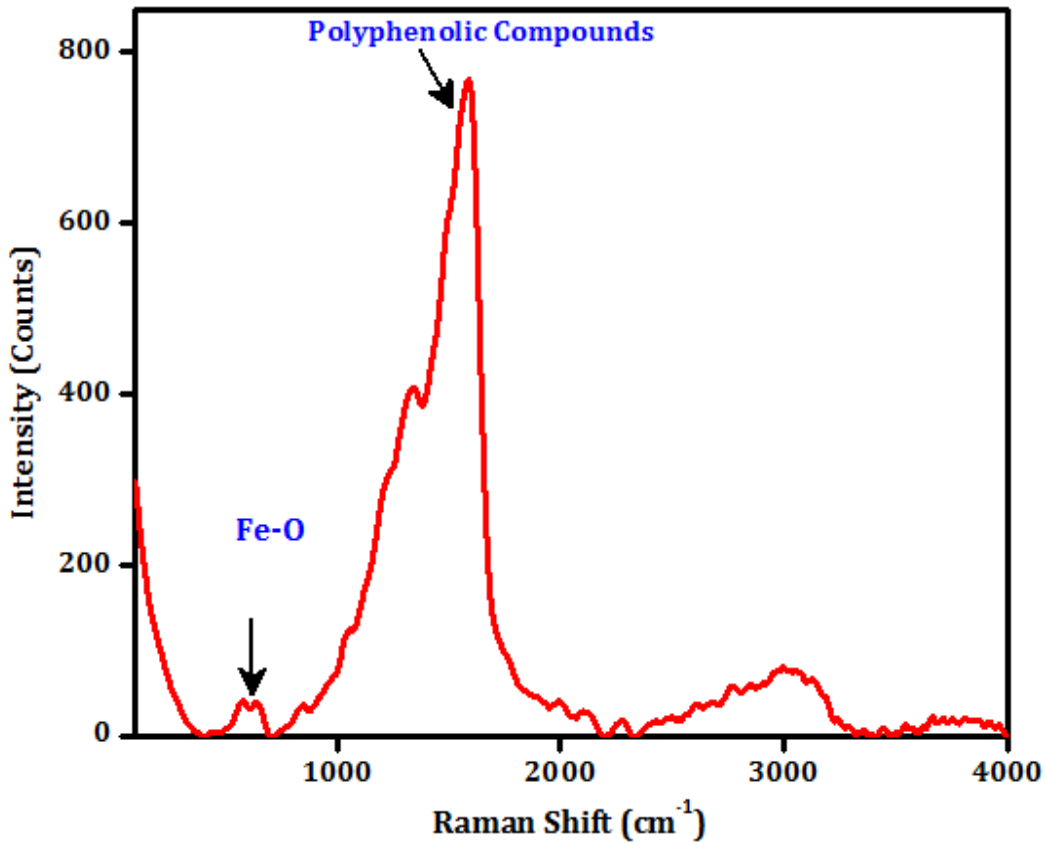

Figure 6. *Raman spectrum of iron nanoparticles.*

The preparation of iron nanoparticles confirmed by the adding eucalyptus leaf extracts in the $FeSO_4.7H_2O$ solution, which resulted in color changes. It indicates the surface plasmon resonance induced due to the prepared nanostructures [28-30].

The presence of iron was also evidenced EDX spectrum as is shown in Figure 7. Because, the extract coated metal nanoparticles reduced as the metallic ions and stabilized the nanoparticles [31].

According to the various researchers, these reduced and stabilized metallic nanoparticles could attribute to the formation of various polyphenolic compounds such as flavonoids, and phenolic acids.

3.5 Raman Spectroscopy

Raman spectroscopy was performed to know the vibrational modes as shown in **Figure 6.** Raman study shows two main peaks centered at 575 and 1583.6 cm^{-1}. The broader and prominent peak noticed at 1583.6 cm^{-1}, represents the aromatic rings of polyphenolic-based compounds [31-35].

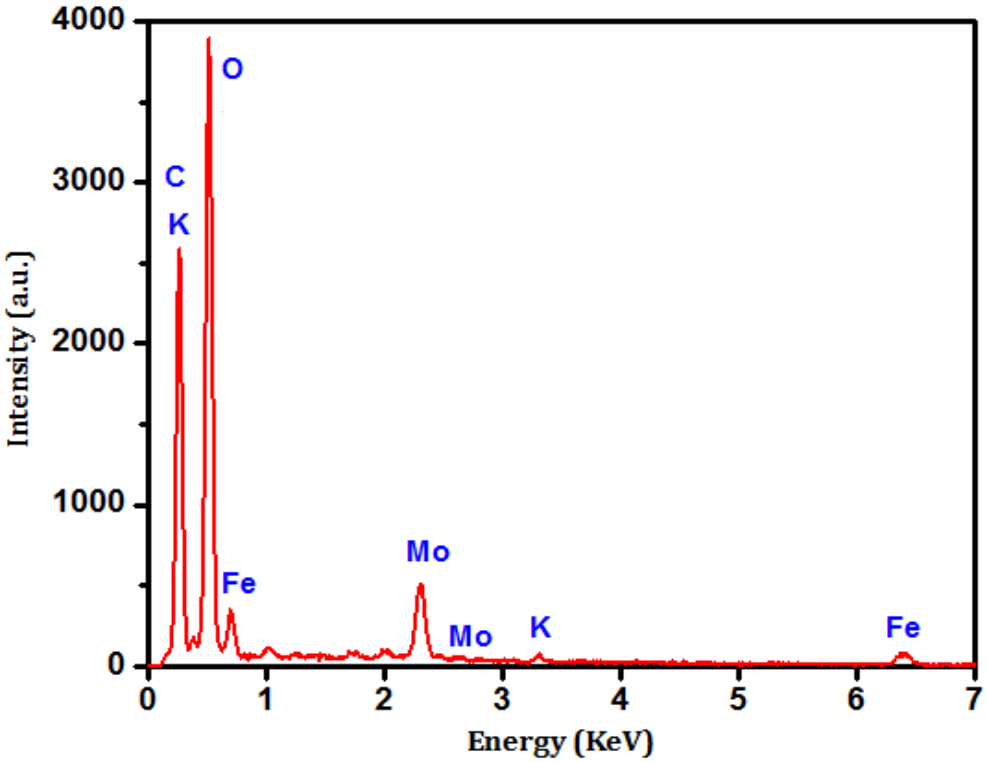

Figure 7. *EDX Spectrum of iron nanoparticles.*

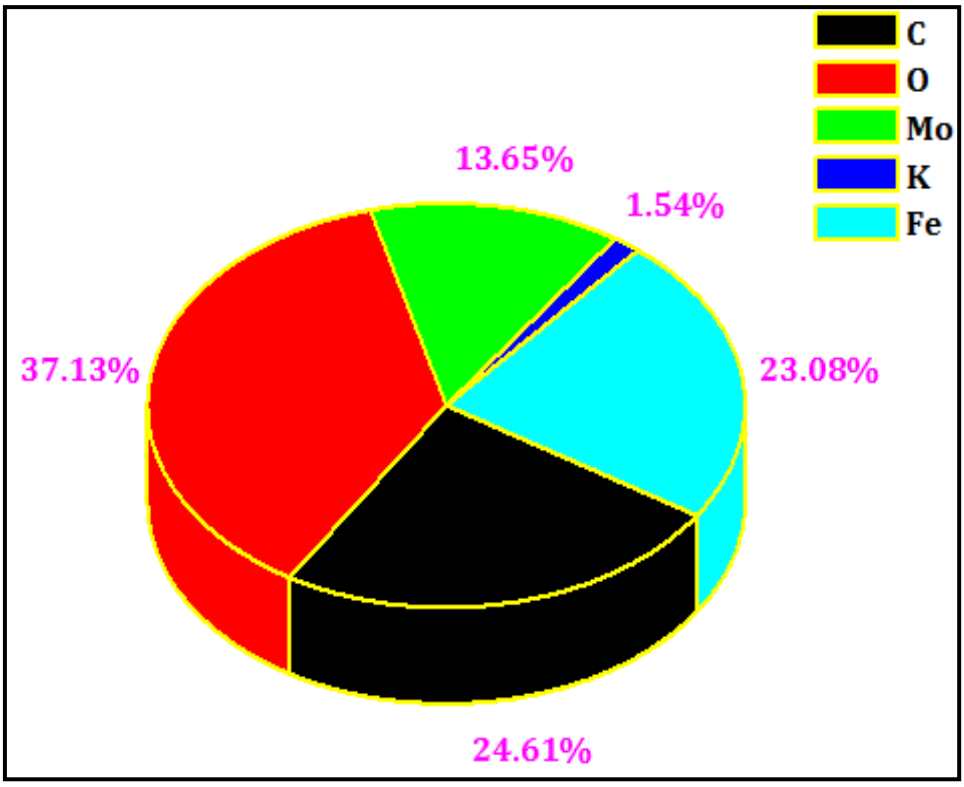

Figure 8. *The pie chart of the weight percentage of sample elements.*

The broader shoulder peak at 575 cm^{-1} corresponds to the Fe-O stretching vibration modes [36].

3.7 Energy Dispersive X-ray Spectroscopy (EDX)

We have investigated the composition and element present in the sample using EDX spectroscopy. The EDX spectrum revealed the presence of 'Fe' and 'O' in the samples, as shown in **Figure 7.** Also, the presented sample elements are depicted in **Figure 8.** Majorly, iron (Fe) and oxygen (O) presence are highest as compare the other elements (impurities are C, Mo, and K). The oxygen presence is high due to environmental issue.

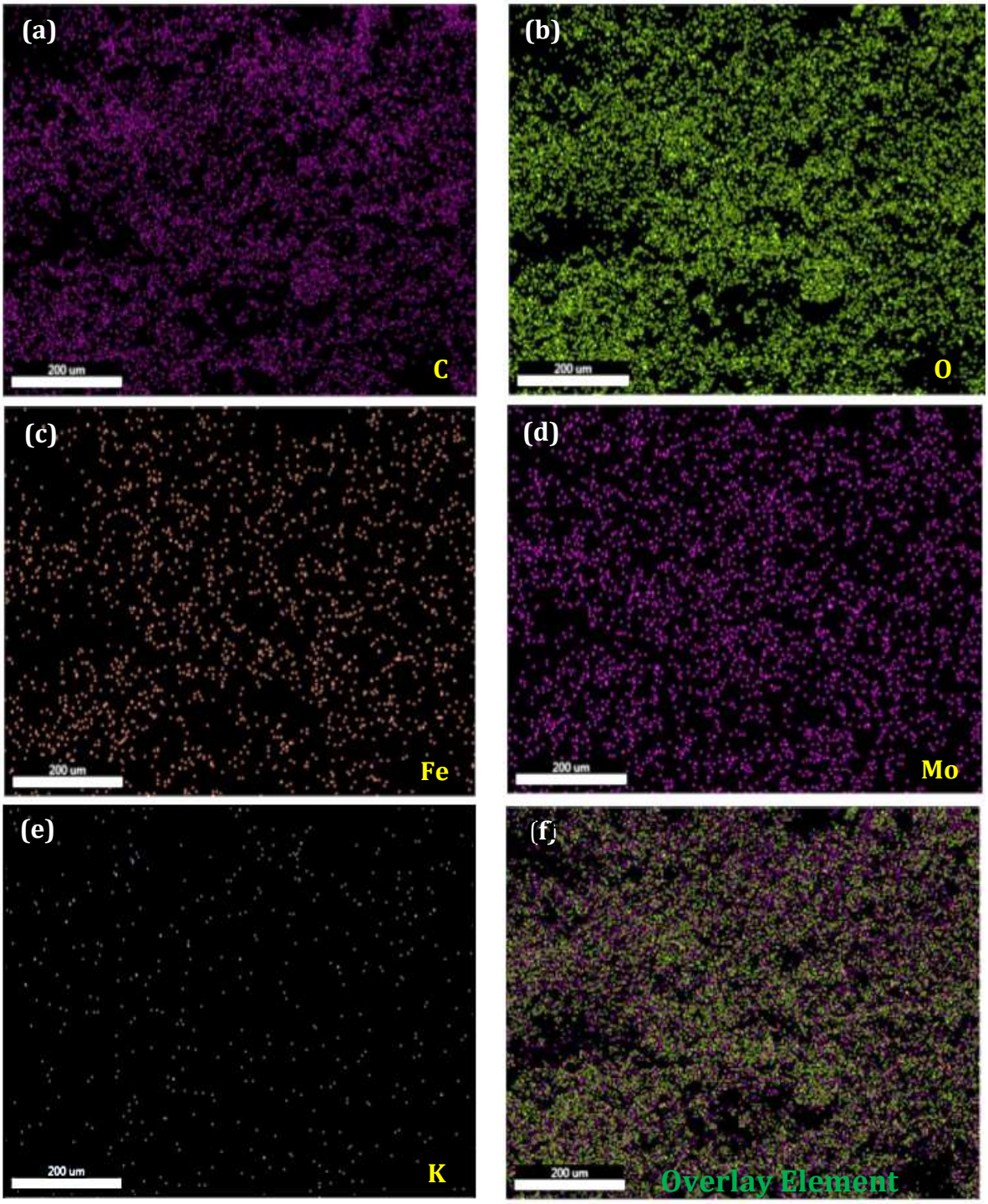

Figure 9. *EDX element mapping (a)-(e) and the pie chart (f) of sample elements.*

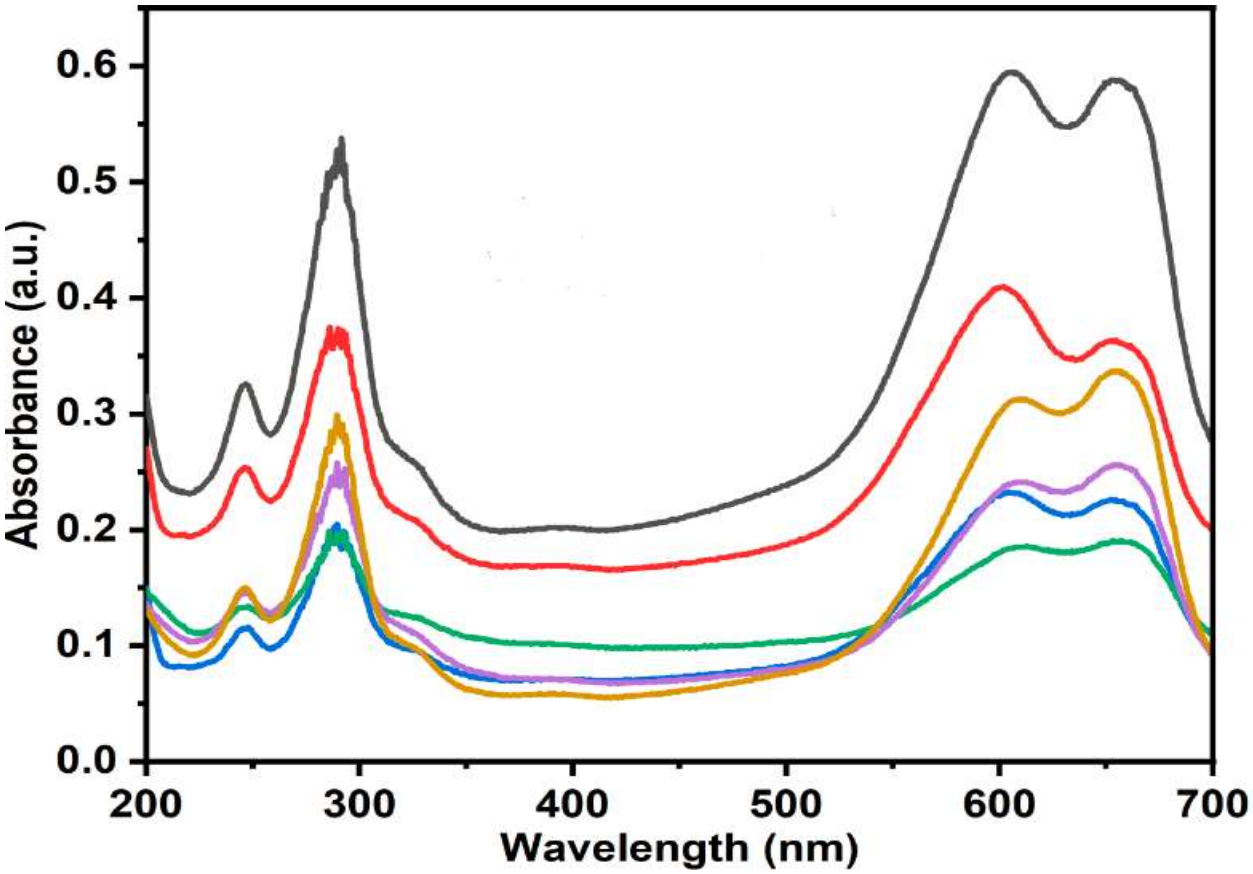

Figure 10. *Photocatalytic activity of green synthesis of iron nanoparticles.*

In addition, the impurities of Mo, C, and K obtained from the Eucalyptus Leaf extracts**.** According to literature, improving the charge separation among the photo generated the charge carriers (electron and hole) and enhancing the photocatalytic performance due to the presence of pollutants [38]. We have performed the EDX mapping of iron nanoparticles, which depicted in **Figure 9 (a)-(e). Figure 9(a), 9(b), 9(c), 9(d)** and 8(e) showed the presence of C, O, Fe, Mo, and K elements, respectively. **Figure 9(f)** demonstrates the overlay mapping of all the elements, which presented with the homogenous distribution within the prepared samples. The presence of other elements along with the iron indicates the partial impurities, which may anticipated in green synthesis process.

3.8 Photocatalytic Performance

To study the photocatalytic activity of green synthesized iron (Fe) nanoparticles, the aqueous based Rhodamine B dye was prepared in which iron nanoparticles added. Further, continuous stirring been maintained for getting a homogeneous solution. This prepared solution was irradiated with ultraviolet and visible light with different interval (0, 30, 60, 90, 120 and 150 min) of time followed by ultraviolet absorption measurement. Usually, the Rhodamine B (RhB) dye has its absorbance peaks at 290 and 585 nm as can be seen here. The green color line shows the maximum absorbance and showed the photocatalytic performance improved up to >98%. Similarly, **Pamela Cristine** et al. reported the photocatalytic performance of Fe_2O_3, with Ti and Ag nanoparticles using RhB under the ultraviolet and visible spectral region. They have shown an improved photocatalytic reduction up to 8% with agglomeration nanoparticles [39]. **Zhang et al.** proposed the better photocatalytic performance under visible spectral region

by using RhB degradation over Bi_2O_3 supported Zn-MoF nanocomposites. The SEM revealed the nanosheet structure and 97.2% of degradation rate of RhB that is useful for wastewater treatment as reported [40].

Figure 10 showed the photocatalytic activity of iron nanoparticles after irradiating of ultraviolet light with the rhodamine B dye. The UV-Vis absorbance recorded in 30 min intervals upon the light exposure. We can see the one sharp absorption peak at 290 nm and another broader peak noticed among 585 to 670 nm. These peaks corresponding to the RhB dye absorption. **Table 1** depicts the different dyes with various nanoparticles and their photocatalytic performance included.

Table 1. *Synthesis of NPs for photocatalytic activity using various dyes*

Plant	NPs	Dyes	Degradation	Ref.
Sambucus ebulus	ZnO	Methyle Blue (MB)	80% in 120 min.	[41]
Azadirachta Indica	Ag-TiO2	MB & RhB	>90% in 120 min.	[42]
Camellia Sinensis	Ni	Crystal violet	99.5	[43]
-	Fe_2O_3	MB& RhB	100 & 98% in 120 min.	[44]

With the increased light irradiation interval time from 0 to 150 min, the absorbance peaks were noticed to be reduced. The decreased absorption of UV-light with the increased time intervals indicates the photo degradation of RhB dye with iron nanoparticles due to catalytic character-istics of the prepared dyes of the polluted water. Under the UV spectrum irradiation, we can also notice the reduced absorbance with respect to timing and peak shifting towards the higher wavelength region. These results indicate the prepared iron nanoparticles ability of Photocatalytic performance, and it depends on the size of the catalyst [3].

4. CONCLUSION

In summary, the iron nanoparticles synthesized by green synthesis method using the eucalyptus leaf extracts. XRD pattern revealed the corresponding peak of iron nanoparticles at Bragg's angle $2\theta=44.3°$. The FTIR and Raman investigations were confirmed the presence of iron stretching vibration at 550 cm^{-1} and 575 cm^{-1}, respectively. The irregular and spherical iron nanoparticles noticed in SEM micrographs. In addition, EDX peak and map shown the presence of iron along with the other natural elements. These nanoparticles and Rhodamine B dye have proven their better photocatalytic performance with the effect of enhanced of time. The prepared iron nanoparticles acted as a good catalyst in the degradation of Rhodamine B dye upon ultraviolet light irradiation. Finally, the green synthesis method is eco-friendly and non-hazardous to produce iron nanoparticles with less efforts.

CONFLICT OF INTEREST

The authors declare that they have no conflict of interest.

REFERENCES

1. Fahmy, H.M., Mohamed, F.M., Marzouq, M.H., EI-Din Mustafa, A.B., Alsoudi, A.M., Ali, O.A., Mohamed, M.A., Mahmoud, F.A., "Review of green methods of iron nanoparticles synthesis and applications", *Bionanoscience*, (2018) 1-13.
2. Jeevanandhan, J., Chan, Y.S., Hung Ku, Y., "Aqueous eucalyptus globules leaf extract-mediated biosynthesis of MgO nanorods", *Appl. Biol. Chem.*, 61 (2018) 197-208.
3. Katta, V. K. M., Dubey, R.S., "Green synthesis of silver nanoparticles using Tagetes erecta plant and investigation of their structural, optical, chemical and morphological properties", *Mater. Today: Proc*., 45 (2021) 794-798.
4. Sundararajan, M., Sailaja, V., John Kennedy, L., Judith Vijaya, J., "Photocatalytic degradation of Rhodamine B under visible light using nanostructures zinc doped cobalt ferrite: Kinetics and mechanism", *Ceram. Int.*, 43 (2017) 540-548.

5. Varadavenkatesan, T., Lyubchik, E., Pai, S., Pugazhendhi, A., Vinayagam, R., Selvaraj,R., "Photocatalytic degradation of Rhodamine B by zinc oxide nanoparticles synthesized using the leaf extract of cyanometra ramiflora", *J. Photochem. Photobiol. B*, 199, (2019) 111621-1-8.
6. Yi, Y., Tu, G., Tsang, E., Xiao, S., Fang, Z., "Green synthesis of iron-based nanoparticles from extracts of Nephrolepis auriculata and applications for Cr(VI) removal", *Mater. Lett.,* 234(2018) 1-12.
7. Ya-yuan Mo, Y., Yan-kui Tang, Wang, S., Ling, J., Zhang, H., Luo, D., "Green synthesis of silver nanoparticles using eucalyptus leaf extract", *Mater. Lett.,* 144(2015) 165-167.
8. Wang, T., Jin, X., Chen, Z., Megharaj, M., Naidu, R., "Green synthesis of Fe nanoparticles using eucalyptus leaf extracts for treatment of eutrophic wastewater", *Sci. Total Environ*., 466-467(2014) 210-213.
9. Vitta, Y., Figueroa, M., Calderon, M., Ciangherotti, C., "Synthesis of iron nanoparticles from aqueous extract of eucalyptus robusta Sm and evaluation of antioxidant and antimicrobial activity", *Materials Science for Energy Technologies*, 3, 97-103(2020).
10. Wang, Z., "Iron complex nanoparticles synthesized by eucalyptus leaves", *ACS Sustain.Chem. Eng.,* 1(12) (2013) 1551-1554.
11. Weng, X.L., Guo, M.Y., Luo, F., Chen, Z.L., "One-step green synthesis of bimetallic Fe/Ni nanoparticles by eucalyptus leaf extract: Biomolecules identification, characterization and catalytic activity", *Chem. Eng.,* 308 (2017) 904-911.
12. Weihua, Xu, T. Yang, S. Liu, L. Du, Q. Chen et al., "Insights into the synthesis, types and application of iron nanoparticles: The overlooked significance of environmental effects", *Environment International*, 158, (2022) 106980.
13. Liu, Y., Jin, X., Chen, Z., "The formation of iron nanoparticles by eucalyptus leaf extract and used to remove Cr(VI)", *Sci. Total Environ*., 627 (2018) 470-479.
14. Umar, K.M., Mandal, B.K., Kumar, K.S., Reddy, P.S., Sreedhar, B., "Biobased green method to synthesise palladium and iron nanoparticles using Terminalia chebula aqueous extract", *Spectrochim Acta A*, 102 (2013) 128-133.
15. Mohan, K.K., Mandal, B.K., Siva, K.K., Sreedhara, P.R., Sreedhar, B., "Biobased green method to synthesise palladium and iron nanoparticles using Terminalia chebula aqueous extract", *Spectrochim Acta A,* 102 (2013) 128-133.
16. Zhang, X., Lin, S., Chen, Z.L., Megharaj, M., Naidu, R., "Kaolinite-supported nanoscale zero valent iron for removal of Pb^{2+} from aqueous solution: Reactivity, characterization and mechanism", *Water Research*, 45 (2011) 3481-3488.
17. Hjiri, M., Zahmouli, N., Khouzami, K., Lassaad, E.M.M., "A Comparison of NO_2 sensing characteristics of a- and y-iron oxide based solid state gas sensors", *Applied Physics A*, 126(10) (2020) 788.
18. Veintemillas-Verdaguer, S., Maria del Puerto Morales, O.B., Miguel, "Colloidal dispersions of maghemite nanoparticles produced by laser Pyrolysis with application as NMR contrast agents", *Journal of Physics D Applied Physics*, 37(15) (2004) 2054.
19. Shukla, S., Jadaun, A., Arora, V., "In vitro toxicity assessment of chitosan oligosaccharide coated iron oxide nanoparticles", Toxicology Reports, 2 (2015) 27-39.
20. Meetei, S.D., Singh, S.D. "Effects of crystal size, structure and quenching on the photoluminescence emission intensity, lifetime and quantum yield of ZrO_2: Eu^{3+} nanocrystals", *J. Lumin.,* 147 (2014) 328.
21. Revathy, J.S., Chitra Priya, N.S., Sandhya, K., Rajendran, D.N., "Structural and Optical Studies of Cerium doped gadolinium oxide phosphor", *Bull. Mater. Sci.,* 44(13) (2021) 1-8.
22. Kanwal, F., Batool, A., Aslam, M., Fatima, A., "Synthesis of coral-like silver chloride-polypyrrole nanocomposites derived from silver nanoparticles and the study of their structural, thermal, optical and electrical properties", *Kuwait J. Sci.,* 48 (2021) 1-11.
23. Vazquez, G., Fontenla, E., Santos, J., Freire, M.S., Gonzalez-Alvarez, J., Antorrena, G., "Antioxidant activity and phenolic content of chestnut (Castanea sativa) shell and eucalyptus (Eucalyptus globulus) bark extracts", *Ind, Crops, Prod*., 28 (2008) 279-285.
24. Das, R.K., Borthakur, B.B., Bora, U., "Green synthesis of gold nanoparticles using ethanolic leaf extract of Centella asiatica", *Mater. Lett.,* 64 (2010) 1445-1447.
25. Iram, M., Guo, C., Guan, Y.P., Ishfaq, A., Liu, H.Z., "Adsorption and magnetic removal of neutral red dye from aqueous solution using Fe_3O_4 hollow nanospheres", *J. Hazard. Mater.,* 181 (2010) 1039-1050.
26. Carroll, K.J., Hudgins, D.M., Spurgeon, S., Kemner, K.M., Mishra, B., Boyanov, M.I., Brown, L.W., Taheri, M.L., Carpenter, E.E., "One-pot aqueous synthesis of Fe and Ag Core/Shell nanoparticles", *Chem. Mater.,* 22 (2010) 6291-6296.
27. Blanco, M.C., Meira, A., Baldomir, D., Rivas, J., Lopezquintela, M.A., "UV-VIS spectra of small iron particles", *IEEE Transactions on Magnetics,* 30 (1994) 739-741.
28. Saravanan, S., "Functional, structural and morphological property of green synthesized silver nanoparticles using azadirachta indica leaf extract", *Materials Today: Proceedings,* 47 (2021) 1815-1818.

29. Shankar, S.S., Rai, A., Ankamwar, B., Singh, A., Ahmad, A., Sastry, M., "Biological synthesis of triangular gold nanoprisms" *J. Nat. Mater.*, 3 (2004) 482-488.
30. Shankar, S.S., Rai, A., Ahmad, A., Sastry, M., "Rapid synthesis of Au, Ag, and bimetallic Au core-Ag shell nanoparticles using Neem (Azadirachta indica) leaf broth", *Colloid. Interface Sci.,* 275 (2004) 496-502.
31. Naseem, T., Farrukh, M.A., "Antibacterial activity of green synthesis of iron nanoparticles using Lawsonia inermis and Gardenia jasminoides leaves extract", *J. Chem.,* (2015) 1-7.
32. Padilla-Cruz, A.L., Garza-Cervantes, J.A., Vasto-Anzaldo, X.G., Garcia-Rivas, G., Leon-Buitimea, A., Morones-Ramirez, J.R., "Synthesis and design of Ag-Fe bimetallic nanoparticles as antimicrobial synergistic combination therapies against clinically relevant pathogens", *Sci. Rep.,* 11 (2021) 5351-1-10.
33. Uddin, R., "HPLC-analysis of polyphenolic compounds in gardenia jasminoides and determination of antioxidant activity by using free radical scavenging assays", *Adv. Pharm. Bull.,* 4 (2014) 273-281.
34. Pompeu, D.R., Larondelle, Y., Roges, H., Abbas, O., Pierna, J.A.F., Baeten, V., "Characterization and discrimination of phenolic compounds using Fourier transform Raman spectroscopy and chemometric tools", *Biotechnolgie Agronmie Societe Environnment,* 22 (2018) 1-16.
35. Ruíz-Baltazar, A., "Structural characterization of Fe–Ag bimetallic nanoparticles synthesized by chemical reduction", *Int. Res. J. Pure Appl. Chem.,* 4 (2014) 263-269.
36. Dong, X.Y., Ji, X.H., Wu, H.L., Zhao, L.L., Li, J., Yang, W.S., "Shape control of silver nanoparticles by stepwise citrate reduction", *J. Phys. Chem. C,* 113 (2009) 6573-6576.
37. Poguberović, S.S., Krčmar, D.M., Maletić, S.P., Kónya, Z., Pilipović, D.D.T., Kerkez, D.V., Rončević, S.D., "Removal of As (III) and Cr(VI) from aqueous solutions using green zero-valent iron nanoparticles produced by oak, mulberry and cherry leaf extracts", *Ecol. Eng.,* 90 (2016) 42-49.
38. Davar, F., Majedi, A., Mirzaei A. "Green synthesis of ZnO nanoparticles and its application in the degradation of some dyes", *J. Am. Ceram. Soc.,* 98(6) (2015) 1739-1746.
39. Cristine, P., Mortari, L.M., Vizzotto S.R., "Iron oxide nanocatalyst with titanium and silver nanoparticles: Synthesis, characterization and photocatalytic activity on the degradation of Rhodamine B dye", *Sci. Rep.,* 10 (2020) 3055.
40. Zhang, Q., Wang, D., Yu, R., Luo, L., Cheng, J., Zhang, Y., "Excellent photocatalytic degradation of rhodamine B over Bi_2O_3 supported on Zn-MOF nanocomposites under visible light", *Green processing and Synthesis*, 12 (2023) 20228123.
41. Alamdari, S., Ghamsari, M.S., Lee, C., "Preparation and Characterization of Zinc Oxide Nanoparticles Using Leaf Extract of Sambucus ebulus", *Appl. Sci.,* 10(10) (2020) 3620.
42. Muneer, M., Kaleem Khan Khosa, M., Akram, N., Khalid, S., Adeel, M., Asif, N., Sherazi, S., "Azadirachta indica leaves extract assisted green synthesis of Ag-TiO_2 for degradation of methylene blue and rhodamine B dyes in aqueous medium", *Green Processing and Synthesis*, 8(1), 659-666.
43. Bibi I., Kamal S., Ahmad A., Iqbal M., Nouren S., Jilani K., "Nickel nanoparticle synthesis using *Camellia Sinensis* as reducing and capping agent: Growth mechanism and photo-catalytic activity evaluation", *Int. J. Bio. Macromol.,* 103 (2017) 783-790.
44. Addalkareem Jasim, S., Kadhim, M.M., Abed Hussein, B., Emad Izzat, S., Mohsen Najm, Z., Chem, C., "Photocatalytic degradation of rhodamine blue using α-Fe_2O_3 nanoparticles", *Phys. Chem. Res.,* 11(1) (2023) 139-147.